Comparative Study of Conducting Polymers by the ESCR Model

T. F. Otero*,† and I. Boyano§

Laboratory of Electrochemistry, Intelligent Materials and Devices, Universidad Politécnica de Cartagena, Paseo Alfonso XIII, 48, 30203 Cartagena, Spain, and Laboratorio Ampliación de Química-Física, Universidad del País Vasco, Paseo Manuel de Lardizábal 3, 20009 San Sebastián, Spain

Received: December 17, 2002

Following the hypothesis of the electrochemically stimulated conformational relaxation model (ESCRM), electrochemically generated films of poly(1-methylpyrrole), polythiophene, poly(3-methylthiophene), polyaniline, and polymethylaniline were studied by potential steps in lithium perchlorate/acetonitrile solutions. All the chronoamperograms studied by influence of different compaction potentials, or different temperatures, show a maximum, indicating the presence of conformational relaxation movements of the polymeric chains as kinetic-controlling processes of the electrochemical oxidation. Magnitudes as charge consumed to compact one mole of polymeric segments during cathodic polarization, the cathodic potential where the compaction of the polymers starts, the enthalpic increment between two stationary states defined by constant overpotentials of compaction and oxidation, and the diffusion constants stated at constant anodic overpotentials were obtained in the context pointed by the model for the studied polymers. The comparative study of the magnitudes for the different polymers, including similar magnitudes for polypyrrole and polyaniline from the literature, allows a comparative view of some structural, kinetic, and thermodynamic aspects, which can be useful for designing tailored properties, or applications, of the conducting polymers.

Introduction

Several theoretical models trying to explain the electrochemical behavior of conducting polymers are available in the literature. In this sense, experimental data can be analyzed by using a diffusional model (Cottrel equation) or, more adequately, by means of migrational models, e.g., the single-pored model of the porous electrode proposed by Posey and Morozumi.[1] Aoki and Tezuka[2−4] simulated chronoamperometric and voltamperometric oxidation curves relying on the assumption that the conductive domain propagates from the metal−polymer interface to the polymer−solution interface. Feldberg[5] introduced capacitative currents to explain voltammetric results, extensive compared to other electrochemical results. Another type of mathematical model able to simulate cyclic voltamperograms of polypyrrole on a rotating disk electrode, the White and coworkers model,[6,7] is based on the conservation of mass and charge along the different regions of the electrode The polypyrrole film is treated as a porous electrode with a high surface-to-volume ratio and a large amount of oxidized film, in a way similar to Feldberg's model. Hillman el al.[8] pointed to the necessity of separating thermodynamic and kinetic phenomena during switching. They proposed a nonquantitative kinetic mechanism of many elementary steps to produce regions of pure-oxidized species from fully reduced regions. Kaplin[9] proposed a model for charge-transfer-controlled redox switching. Peter and co-workers[10] suggested that redox switching could be modeled in terms of an instantaneous two-dimensional nucleation and growth model.

All those models assume that electrochemical responses of conducting polymers are unable to provide information about structural and polymeric changes in the film. They do not take into account reversible changes in volume, swelling, and shrinking during oxidation and reduction processes[11,12] which originate devices such as artificial muscles.[13−16] The electrochemically stimulated conformational relaxation model (ESCR) model was established[17−20] on the hypothesis that when a film of polypyrrole is oxidized by an anodic polarization, electrons are extracted from the polymeric chains, generating positive polarons and bipolarons, reorganizing double bonds and angles between monomeric units, and giving rise to conformational movements. Free volume is generated, and counterions and solvent penetrate by diffusion control from the solution and the polymer swells. If the oxidized polymer is reduced by a potential sweep, opposite processes take place and the polymer shrinks. Meanwhile, counterions move toward the solution by diffusion control.[21,22] This process can be described as:

$$(\text{neutral polymer})_s + n\text{ClO}_{4\text{solv}}^- \underset{\text{reduction}}{\overset{\text{oxidation}}{\rightleftharpoons}} [(\text{polymer})^{n+}(\text{ClO}_4^-)_n]_{\text{gel}} + ne^-$$

Considering that the polymer is shrinking along a reduction process, diffusion of counterions toward the solution becomes more and more difficult, and the cathodic current required to reduce the polymer decreases but does not drop to zero. As the shrinking process continues, the structure of the polymer is closed before the reduction process is completed. Now the counterions need to open a way in a more dense entanglement by conformational movements of the polymeric chains; the process requires long times or high overpotentials under conformational kinetic control.[23,24] This flow of counterions induces a denser compaction, as in electroosmotic processes (Figure 1). Along the voltammetric sweep, the potential of transition between diffusion and conformational relaxation control is defined as the closing potential.

† Universidad Politécnica de Cartagena.
§ Universidad del País Vasco.

10.1021/jp027748j CCC: $25.00 © 2003 American Chemical Society
Published on Web 06/24/2003

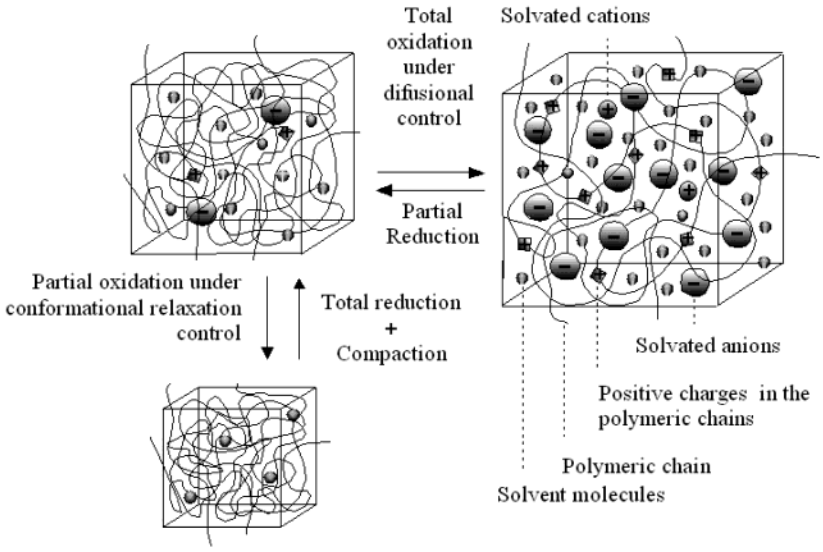

Figure 1. Schematic representation of the reversible variation of volume associated with the electrochemical-switching conducting polymers. Changes in free volume are mainly due to two effects: electrostatic repulsions between fixed positive charges and exchange of cations, anions, and solvent molecules between the polymer and the solution.

When the polymer was reduced by polarization at a potential more anodic than the closing potential, any subsequent oxidation occurs under uniform diffusion control of the penetrating counterions. After reduction and compaction of the structure at a potential more cathodic than the closing potential, the subsequent oxidation requires the stimulation of local (on a different nucleus) conformational relaxations, opening the structure and allowing the penetration of counterions; the oxidation kinetics is under relaxation-nucleation control. The nucleation process was proved by formation of a black nucleus of oxidized polypyrrole in a yellow-reduced film.[25] The oxidation of a compacted film by a potential step originates a maximum on the chronoamperometric response. The oxidation of a noncompacted film gives rise to a continuous exponential decrease of the current.

The compaction degree is influenced by different experimental variables: the compaction potential, the polarization time at this compaction potential, electrolyte concentration, and the temperature. By the ESCR model, conformational relaxation, nucleation, and diffusion kinetics were quantified, giving self-consistent chronoamperometric, voltammetric, and chronocoulometric equations able to simulate the influence of the different variables on the experimental responses from polypyrrole or polyaniline.

Previous studies pointing out the influence of the polarization time (wait time) at high-cathodic potentials of prepolarization on the shape of anodic chronoamperograms,[26,27] voltammograms,[28] and the existence of first-scan effects[29] had already suggested the existence and control of structural changes in the solid matrix during electrochemical responses.

The aim of this work is to check if the model can be extended to other conducting polymers such as poly(1-methylpyrrole), polythiophene, poly(3-methylthiophene), and polymethylaniline films. Considering also previous studies using polypyrrole and polyaniline films, we will have results from three basic polymers: polypyrrole, polythiophene, and polyaniline and from a methyl-substituted polymer from every family of the basic polymers. (Figure 2).

The goal is to check if the model can provide us with some information about the influence of the molecular structure on the polymeric oxidation, providing us with some comparative magnitudes between different conducting polymers.

Experimental Methods

Polymer films were electropolymerized and checked in a one-compartment electrochemical cell connected to a PAR M270 potentiostat−galvanostat controlled from a PC. The working electrode and counter electrode were platinum sheets having 1- and 4 cm^2 of surface area, respectively. A saturated calomel electrode (SCE) from Crison Instruments was used as the reference electrode. Monomers (pyrrol, Aldrich 98%; 1-methylpyrrol, Fluka 98+%; aniline, Merck for analyses, methyl aniline, Aldrich 98%; thiophene, Janssen 99+%; and 3-methylthiophene, Janssen 99+%) were distilled under vacuum before use and stored under N_2 at −10 °C. Acetonitrile (Lab Scan, HPLC grade), anhydrous lithium perchlorate (Aldrich, 99%), and sulfuric acid (Merck, 95−97% content) were used as received. All the solutions were deareated by bubbling N_2 for 10 min before the current flow.

Results

Polymer films were generated electrochemically by flow of 50 mC cm^{-2} throughout a monomeric solution. Three different methods were used to generate the studied polymer films: (1) at constant potential: polypyrrole and poly(1-methylpyrrole) were generated at a constant potential of 700 mV in 0.2 M $LiClO_4$ + 0.1 M monomer (pyrrole or 1-methylpyrrole) acetonitrile solution; (2) by consecutive square waves of potential: 3 s at −300 mV followed by 8 s at 700 mV and back to −300 mV until the overall polymerization charge (oxidation minus reduction charge) was completed; polythiophene and poly(3-methylthiophene) were generated in 0.2 M $LiClO_4$ + 0.1 M monomer (thiophene or 3-methylthiophene) acetonitrile solution by potential steps; (3) by potential cycling: polyaniline and polymethylaniline films were grown by potential cycling at 50 mV s^{-1} between −100 and 900 mV in 0.2 M aniline + 0.1 M H_2SO_4 aqueous solutions until the overall polymerization charge was completed.

Films showing electrochromic properties were obtained (transparent in the reduced state and dark under oxidized state). After generation, each polymer-coated electrode was rinsed with acetonitrile and transferred to the control solution (0.1 M lithium perchlorate/acetonitrile solution) where the films were submitted to chronoamperometric analysis. The polymer was reduced to

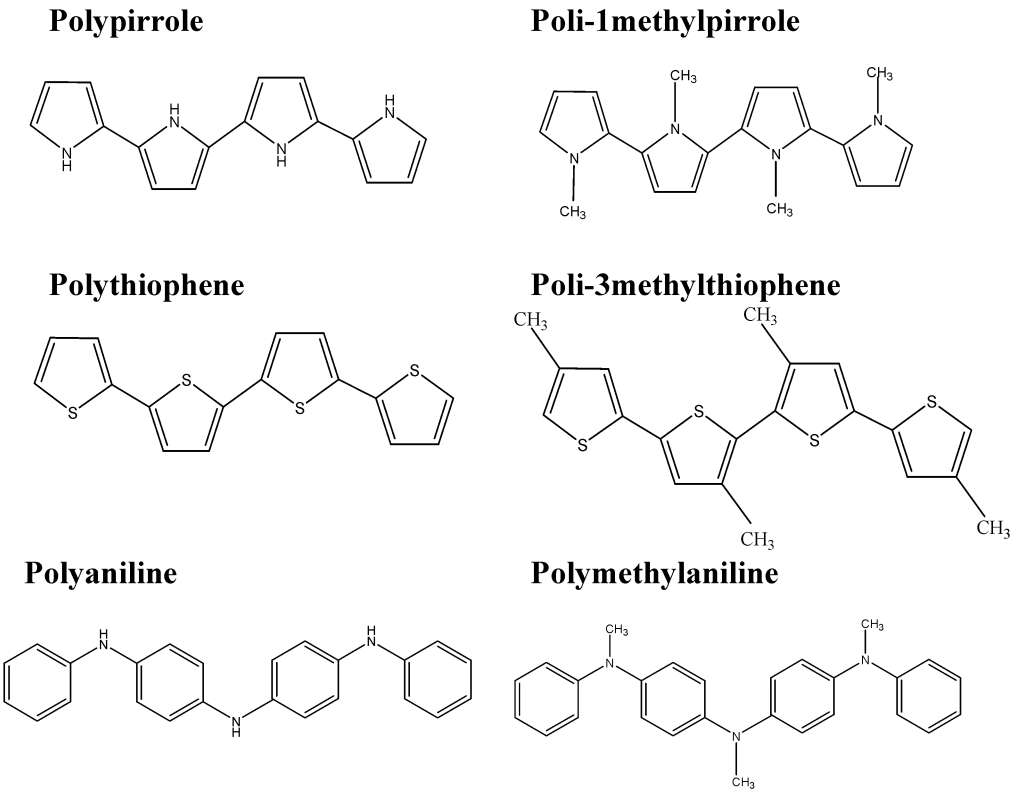

Figure 2. Schematic structure of polymers used in this work.

an initial potential (E_c) for 1 min. Then the potential was stepped to an oxidation potential (E). Chronoamperometric responses were obtained from different reduction potentials, to different anodic potentials, and at different temperatures. The procedure was repeated twice for every value of the studied variable to check the reproducibility of the chronoamperogram. Reproducibilities greater than 99% were obtained. Those experimental results will be used to obtain different constants, specific for every conducting polymer and defined by the ESCR model. A comparative study and discussion of those constants could be a way to obtain comparative structural information and quantification of those polymers.

Theoretical Background and Goals. The rate at which conformational changes occur in a conducting polymer film immersed in an electrolytic media are assumed to depend, as in other relaxation models, on structural and electrochemical variables through an Arrhenius type law.[18]

$$\tau = \tau_0 \exp\frac{\Delta H}{RT} = \tau_0 \exp\left[\frac{\Delta H^* + z_c(E_s - E_c) - z_r(E - E_0)}{RT}\right] \quad (1)$$

The conformational relaxation time (τ) is defined as the time required to change the conformation of a polymeric segment, previously submitted to a cathodic prepolarization and compaction (E_c) when it is oxidized by potential step to an anodic potential (E) at a given temperature (T), allowing the penetration of counterions. A polymeric segment is considered here as the minimum chain length whose conformational changes allow ionic interchanges between the polymer and the solution. ΔH is the energy required for relaxing one mole of segments between two stationary states, as in any other conformational model. To describe the electrochemistry of the conducting polymers, this enthalpy includes three components: ΔH^* is the enthalpic increment of the system between two different stationary states, i.e., compacted and oxidized, in the absence of any external electric field; $z_c(E_s - E_c)$ is the electrochemical energy required to reduce, close, and compact one mole of polymeric segments by cathodic polarization; and $z_r(E - E_0)$ is the electrochemical energy required to relax and oxidize one mole of compacted polymeric segments. The constant z_c is defined as the charge required to reduce, close, and compact one mole of polymeric segments. The closure and compaction of the polymeric matrix is proportional to a cathodic overpotential ($\eta_c = E_s - E_c$), where E_s is the experimental potential of closure and E_c is the compaction potential. In this context, by starting a potential step from a potential more anodic than E_s, the polymeric structure is relaxed, and any subsequent oxidation will not be controlled by energetic requirements to open the polymeric network but by counterion diffusion across the open structure. Finally, the energy required to relax one mole of compacted polymeric segments is supplied when an anodic overpotential ($\eta = E - E_0$), referred to that potential where the oxidation of a relaxed conducting polymer begins (E_0), is applied to the compacted polymer (Figure 3). The new constant z_r is defined as the coefficient of electrochemical relaxation, that is, the charge consumed to relax one mole of compacted polymeric segments.

The ESCR model establishes that the conformational relaxation processes in conducting polymers are under the control of the chemical (solvent and concentration of the electrolyte) and energetic (cathodic overpotential, anodic overpotential, and temperature) variables. The model provides a self-consistent mathematical description (without any adjustable parameter) of chronoamperograms,[18,25] chronocoulograms,[30] and voltammograms[31] performed under conformational relaxation control with polypyrrole films. The experimental results can be predicted and simulated as a function of the different chemical or electrical variables. To check if the model can be applied to different

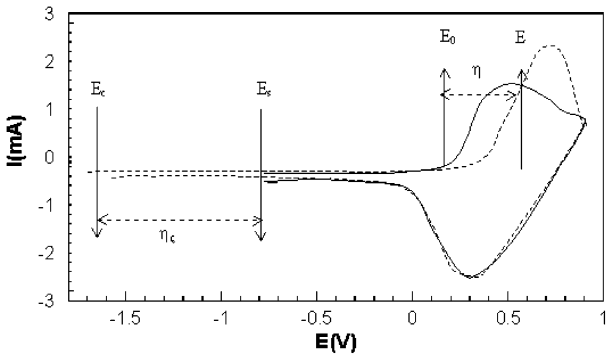

Figure 3. Voltamograms performed from −1800 mV, kept for 60 s and 800 mV at 20 mV/s in 0.2 M $LiClO_4$/acetonitrile solution (− − − −), applied to a film poly(1-methylpyrrole) and from −800 and 800 mV (—). E_s is the closing potential, E_c the potential of polarization, η_c closing overpotential, E_o the starting oxidation potential for a noncompacted film; any polarization at an anodic potential more anodic than E originates an oxidation overpotential: η.

conducting polymers, it was extended to films of polyaniline,[32] where the interchange of protons and anions can interfere. Our aim now is extending the model to different conducting polymers, obtaining their basic constants to try to attain a comparative quantification between them and, if possible, to obtain quantitative structural information. Thus, the energy required to close and compact one mole of segments, or the energy needed to relax and oxidize one mole of compacted segments, must be related to the molecular structure of the studied chains. In this initial approach, we will choose three families of conducting polymers, polypyrrole, polyaniline, and polythiophene, and study the basic polymers (constants from polypyrrole and polyaniline are already available from previous papers) and a methyl-substituted polymer from every family.

To obtain the different constants, the model predicted a semilogarithmic dependence[25] of the times for the chronoamperometric maxima as a function of the different experimental variables as compaction and oxidation overpotentials and reverse temperature (eq 2).

$$\ln \tau_{max} = C_1 + \frac{\Delta H^*}{RT} + \frac{z_c}{RT}\eta_c - \frac{z_r}{RT}\eta \qquad (2)$$

Obtention of z_c and E_s for the Different Polymers. In the context of the ESCR model, z_c is the coefficient of cathodic compaction, that is, the charge spent to compact one mole of polymeric segments. E_s is the closing potential; the polymer shrinks during reduction along a cathodic potential sweep, and the counterions diffuse toward the solution before E_s is attained. After E_s, the counterions are expulsed (and the reduction is completed) under control of the conformational polymeric movements. This requires high energy (high overpotentials) or long reduction times. The subsequent oxidation by a potential step gives chronoamperograms showing a maximum because the conformational movements start on different nuclei, where the mobility of the chains is greater.

The model predicts that the times for the maxima for the different chronoamperograms have a semilogarithmic dependence (eq 2) on the cathodic potential of prepolarization and closing of the structure. Therfore, experiments were performed keeping constant the temperature, concentration of the electrolyte, and oxidation overpotential, thus transforming eq 2 into:

$$\ln \tau_{max} = C' - \frac{z_c \eta_c}{RT} \qquad (3)$$

and z_c can be obtained for every polymer from the slope of the semilogarithmic plot.

Experimental chronoamperograms obtained following the above procedure can be observed in Figure 4 for: polythiophene (Figure 4a), poly(3-methylthiophene) (Figure 4b), polymethylaniline (Figure 4c), and poly(1-methylpyrrole) (Figure 4d). Results for polypyrrole[33] and polyaniline[32] were published in previous papers. All the chronoamperograms were performed at 25 °C in 0.1 $LiClO_4$/acetonitrile solutions. The potential steps were performed from the different cathodic potentials shown in the figure, maintaining the cathodic polarization for 60 s to the same anodic potential for each polymer (800 mV for polythiophene, 900 mV for poly(3-methylthiophene), 400 mV for polymethylaniline, and 300 mV for poly(1-methylpyrrole)). All the experimental chronoamperograms show a maximum, as predicted by the ESCR model when the polymer was compacted by polarization at an initial potential more cathodic than the closing potential. A semilogarithmic variation of those experimental τ_{max} values with the initial potential of reduction was obtained for every studied conducting polymer. Figure 4e shows that variation for a poly(1-methylpyrrole) film. Table 1 shows slopes and correlation coefficients of the semilogarithmic variations obtained for the different studied polymers. Every slope allows us to obtain the constant z_r for the concomitant conducting polymer (Table 1).

On the other hand, when the polymeric film is reduced under constant temperature and constant concentration of electrolyte, taking into account eq 2, E_s is the lower initial potential of reduction, giving a maximum on the subsequent anodic chronoamperogram. E_s can be obtained by extrapolation of the semilogarithmic evolution of the maxima at low times (a time for the maximum (shoulder in this case) low enough that it cannot be measured under our experimental conditions, i.e., 0.1 s). Table 1 shows the obtained E_s values for the studied polymers.

Those results indicate, as expected, that every methyl-substituted polymer requires a higher energy to compact one mole of polymeric segments than the nonsubstituted polymer of the same family. The presence of a lateral chemical group induces difficulties to compact the film.

The closing potential (E_s) shifts to more cathodic values in substituted polymers, related to the closing potentials for the nonsubstituted ones of the same family. That is, under constant temperature and constant concentration of the electrolyte, a higher potential gradient is required across the film to reduce and close the structure of the substituted polymers. As similar small cathodic currents flow by the system at the compaction potential, higher electrical work is required to reduce and close substituted polymers from every one of the studied families. The presence of the lateral group makes the compaction of the chains difficult, and the expulsion of a counterion along a voltammetric reduction undergoes diffusion control until potentials are more cathodic.

According to E_s, the studied families can be classified from low potential gradients to higher potential gradients across the film to close the structure: polythiophene < polyaniline < polypyrrole. The methyl group induces a cathodic potential shift ranging from 300 to 400 mV, related to the nonsubstituted polymer.

Once the structure is closed, the reduction−compaction is completed under conformational relaxation control, and the charge consumed to compact one mole of polymeric segments (z_c) is higher in methyl-substituted polymers. That means that the more cathodic the closing potential of the substituted

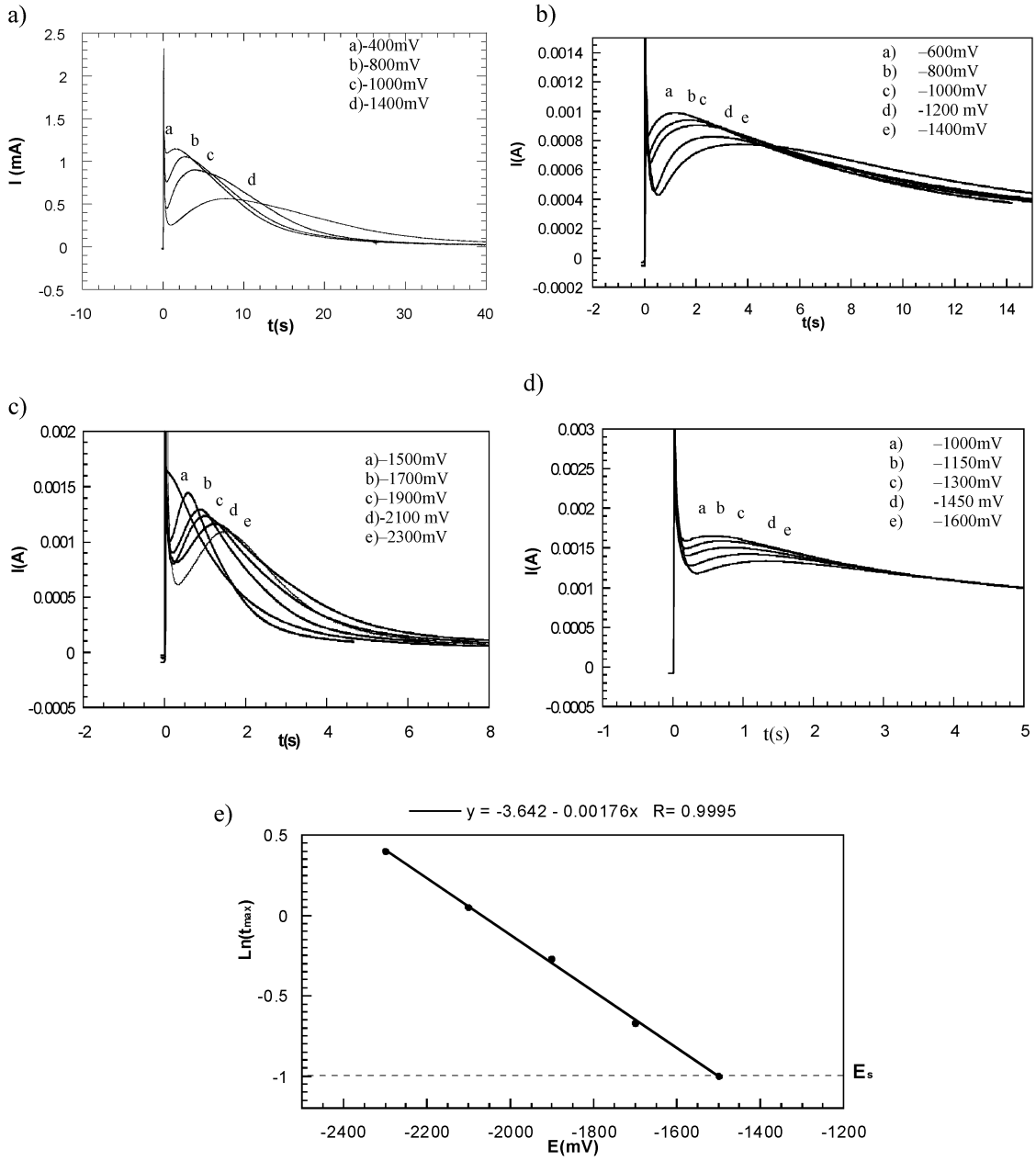

Figure 4. (a) Chronoamperograms of polythiophene film stepped from different potentials of prepolarization (−400, −800, −1000, and 1400 mV vs SCE) to the same anodic limits (800 mV) at constant temperature (25 °C) in 0.1 M $LiClO_4$/acetonitrile solution. This chronoamperogram shows maxima necessary to obtain the z_r constant. (b) Chronoamperograms of poly(3-methylthiophene) film stepped from different potentials of prepolarization during 60 s (−600, −800, −1000 , −1200, and −1400 mV) to the same anodic limits (900 mV). (c) Chronoamperograms of poly(1-methylpyrrole) film stepped from different potentials of prepolarization during 60 s (−1500, −1700, −1900, −2100, and 2300 mV vs SCE) to the same anodic limits (300 mV). (d) Chronoamperograms of polymethylaniline film stepped from different potentials of prepolarization during 60 s (−1000, −1150, −1300, −1450, and −1600 mV vs SCE) to the same anodic limits (400 mV). (e) Semilogarithmic plot of ln τ_{max} vs lower potential for poly(1-methylpyrrole). The coefficient of cathodic polarization z_r for poly(1-methylpyrrole) was calculated from the slope's end. E_s is the potential at which ln (τ_{max}) is −1.

polymers is, the structure is closed when the polymer keeps a higher oxidation degree, thus trapping more counterions inside the film per mole of segments.

According to the charge consumed to compact one mole of polymeric segments, z_c, we have polythiophene < polypyrrole < polyaniline. The gap between unsubstituted and substituted polymers increases in the same way from 800 to 1400 $C \cdot mol^{-1}$.

Molar Enthalpies, ΔH. A similar experimental procedure was repeated, keeping constant the electrical and chemical variables and changing the temperature for every experiment to get the increment in molar polymeric enthalpy, ΔH, between two different states.

TABLE 1: Values of z_c and E_s for Different Conducting Polymers

polymer	slope	*r* (correlation coefficient)	z_c ($C\ mol^{-1}$)	E_s (mV)
polythiophene	1.0874	0.992	2692.8	−300
poly(3-methylthiophene)	1.4169	0.993	3508.8	−600
polypyrrole	1.4049	0.993	3479.1	−900
poly(1-methylpyrrole)	1.7600	0.999	4358.4	−1500
polyaniline	2.2363	0.996	5537.9	−550
polymethylaniline	2.8000	0.999	6933.9	−900

According to eq 1, we have to perform potential steps from an established cathodic potential, more cathodic than the closing

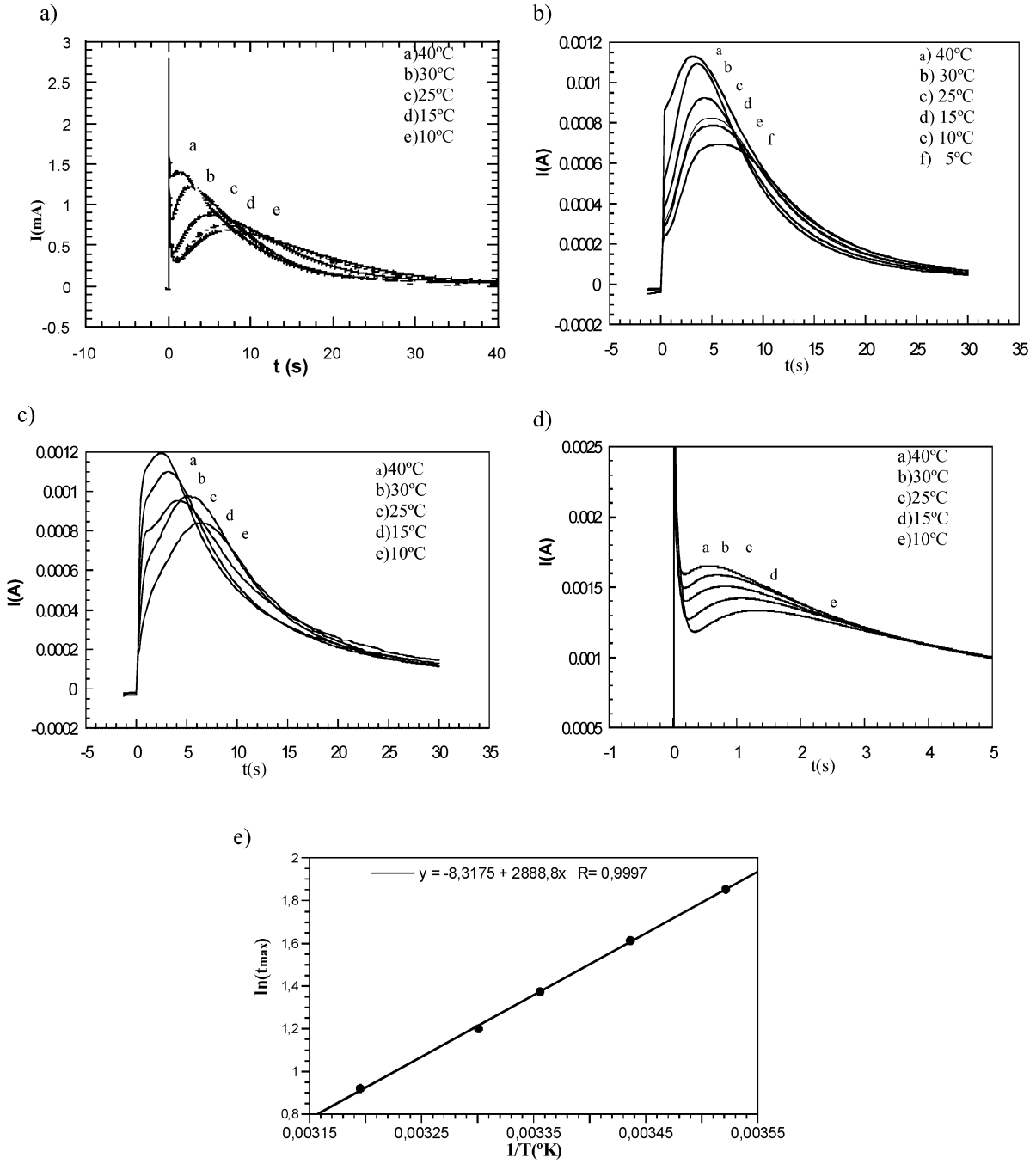

Figure 5. (a) Chronoamperograms performed to a polythiophene film at the same potential step (−600 mV for cathodic potential (maintained during 60 s) and 800 anodic potential) at different temperatures (40, 30, 25, 15, and 10 °C). This chronoamperogram shows the maxima necessary to obtain the ΔH constant temperature in 0.1 M $LiClO_4$/acetonitrile solution. (b) Chronoamperograms of a poly(3-methylthiophene) film at the same potential step (−900 mV for cathodic potential (maintained during 60 s) and 900 anodic potential) at different temperatures (40, 30, 25, 15, 10, and 5 °C). (c) Chronoamperograms of a poly(1-methylpyrrole) film at the same potential step (−1800 mV for cathodic potential (maintained during 60 s) and 300 anodic potential) at different temperatures (40, 30, 25, 15, and 10 °C). (d) Chronoamperograms of a polyaniline film at the same potential step (−1300 mV for cathodic potential (maintained during 60 s) and 400 anodic potential) at different temperatures (40, 30, 25, 15, and 10 °C). (e) Representation of ln τ_{max} vs $1/T$. The conformational energy consumed per mole of polymeric (ΔH) for polythiophene film can be obtained from the slope, following eq 3.

potential, maintained for a constant time of 60 s to the same anodic potential in 0.1 M $LiClO_4$/acetonitrile solutions, changing the temperature of the electrochemical bath for consecutive experiments. Under those conditions eq 2 becomes:

$$\ln \tau_{max} = C''' - \frac{\Delta H^*}{RT} \qquad (4)$$

The obtained experimental chronoamperograms can be observed in Figure 5 for the different studied polymers, polythiophene (Figure 5a), poly(3-methylthiophene) (Figure 5b), polymethylaniline (Figure 5c), and poly(1-methylpyrrole) (Figure 5d), using experimental temperatures ranging between 5 and 40 °C, as can be observed in every figure. The experimental chronoamperograms using electrogenerated films of polyaniline or polypyrrole were presented in previous papers.[32,33] Each polymer film was polarized at a constant cathodic potential (E_c) (−600 mV for polythiophene, −900 mV for poly(3-methylthiophene), −1800 mV for poly(1-methylpyrrole), and −1300

TABLE 2: Values of ΔH for Different Conducting Polymers

polymer	slope	R (correlation coefficient)	ΔH (kJ/mol)
polypyrrole	3.369	0.993	28
poly(1-methylpyrrole)	2.082	0.999	17.3
polyaniline	1.733	0.997	14.4
polymethylaniline	1.215	0.996	10.1
polythiophene	2.888	0.99	24
poly(3-methyltiofene)	1.901	0.999	15.8

mV for polymethylaniline) for 60 s at ambient temperature. All those potentials are 300 mV more cathodic than the closing potential (E_s) of each polymer. Thus, we maintain a constant cathodic overpotential ($\eta_c = E_c - E_s = -300$ mV), and every film will be compacted for the same time and at the same overpotential. Then the temperature was increased until the experimental values, and then the potential was stepped to an anodic potential able to oxidize the polymer (800 mV for polythiophene, 900 mV for poly(3-methylthiophene), 300 mV for poly(1-methylpyrrole), and 400 mV for polymethylaniline). All the obtained experimental chronoamperograms show the maxima indicating the conformational relaxation control of the oxidation kinetics. Plotting the times of those maxima versus the reverse temperature, we obtained a linear dependence and were able to deduce ΔH from the slope. Figure 5e shows the linear variation obtained from the polythiophene film. Slopes and correlation coefficients of the linear variations obtained for the studied films as well as the obtained molar enthalpies ΔH can be observed in Table 2.

ΔH means the increment of the conformational relaxation energy involved per mole of polymeric segments including both chemical (ΔH^*) and electrochemical ($z_c\eta_c$ and $z_r\eta$) components. Those results show lower ΔH from the methylated polymers than from the unsubstituted ones and increasing values in the following order for the studied families: polyaniline < polythyophene < polypyrrole. ΔH includes changes in conformational energies, polymer−polymer, polymer−solvent, and polymer−ions interactions between two stationary states, reduced (compacted) and oxidized (expanded). Low values indicate wake changes of those internal energies during the process.

In this context, the obtained ΔH almost correlates with reverse experimental closing potentials (E_s) because lower internal ΔH requires a higher external work (higher cathodic potentials with similar current densities at constant temperature) to close the polymeric structure along a reducing potential sweep, i.e., polymethylaniline, $\Delta H = 10.1$ kJ/mol; $E_s = -1500$ mV. On the other side, strong internal energetic changes during the process require lower external electric potentials to close the structure, i.e., polypyrrole: $\Delta H = 28$ kJ/mol; $E_s = -300$ mV. Those energetic changes also could play important roles to optimize the electrochemical properties of the conducting polymers and their applications, such as electrochemomechanical, energy storage, electrochromic, electroporosity, electron−ion transduction, etc. In this context, we will compare in a future paper ΔH obtained from artificial muscles, relaxation processes, and other electrochemical properties.

***"b"* Diffusion Constant.** Relaxation processes were avoided when the experimental potential steps were initiated at a more anodic potential than the closing potential (between E_s and E_0), and the oxidation takes place under diffusion control. The flow of charge is under control of the diffusion of counterions required to keep the electroneutrality inside the film. The evolution of the current under those conditions is[18]

$$I_d(\tau) = bQ_d e^{-b\tau} \quad (5)$$

$$Q_d(\tau) = Q_d[1 - e^{-b\tau}] \quad (6)$$

where b is related to the diffusion coefficient. Rearranging and taking logarithms:

$$\ln\left[1 - \frac{Q_d(\tau)}{Q_d}\right] = -b\tau \quad (7)$$

Chronoamperograms were performed at 25 °C in 0.1 M $LiClO_4$/acetonitrile solution. Potential step starts with a polarization for 60 s to a more anodic potential than E_s (−200 mV for polythiophene (Figure 6a), −500 mV for poly(3-methylthiophene) (Figure 6b), −1400 mV for poly(1-methylpyrrole) (Figure 6c), and −800 mV for polymethylaniline (Figure 6d)). Then the potential was stepped to the different anodic potentials shown in Figure 6. For every polymer, a semilogarithmic plot of $(1 - Q_d(\tau)/Q_d)$ vs the oxidation time allows the constant b to be obtained from the slope. Q_d would be the charge associated with the oxidation process obtained by integration of the chronoamperogram, and $Q_d(\tau)$ would be the charge consumed at each oxidation time.

When the procedure is repeated, stepping the potential to different anodic potentials (for example, with poly(3-methylthiophene) to 500, 600, 700, 800, and 900 mV (Figure 6e)), the variation of the diffusion constant b as a function of the anodic potential is obtained, as can be seen in Figure 6f.

Figure 6e shows that the slope (b) of the experimental curves changes when the oxidation potential changes. A linear variation of b, as a function of the anodic potential was obtained (Figure 6f). The equation of those straightforward variations can be seen for the studied materials in Table 3. In the context of the ESCR model, increasing anodic potentials means faster oxidation and swelling of the polymer film. In a more swollen film, a faster diffusion process occurs.

From b, the diffusion constant (D_{app}) of the counterion in the polymer can be obtained:

$$b = \frac{2D_{app}}{h^2} \quad (8)$$

Like b, the diffusion constant (D_{app}) would be a function of the oxidation potential because the oxidation potential fixes the swelling degree of the polymer matrix. Increasing anodic potentials of polarization, from E_0, controls the oxidation level that produces faster relaxation, nucleation, oxidation, and faster swelling rates. Increasing swelling degrees gives larger distances between polymeric chains, larger pores, and rising mobilities of the counterions inside or outside the polymer.

Because the diffusion constant depends on the compaction and swelling degrees throughout the oxidation degree of each polymer, to compare diffusion constant b from different polymers, a constant anodic overpotential must be chosen for every polymer ($\eta = 200$ mV). The polymer never oxidizes if the anodic potential limit is lower than E_0, and the oxidation overpotential $\eta = E - E_0$.

Taking into account eq 2, E_0 for the studied polymers can be obtained by extrapolation of the semilogarithmic evolution of the maxima as a function of the oxidation potentials at low times (a time for the maxima low enough that it cannot be measured under our experimental conditions, i.e., 0.1 s). The obtained E_0 for the different studied polymers are −350 mV for polypyrrole, −250 mV for poly(1-methylpyrrole), −100 mV for polyaniline,

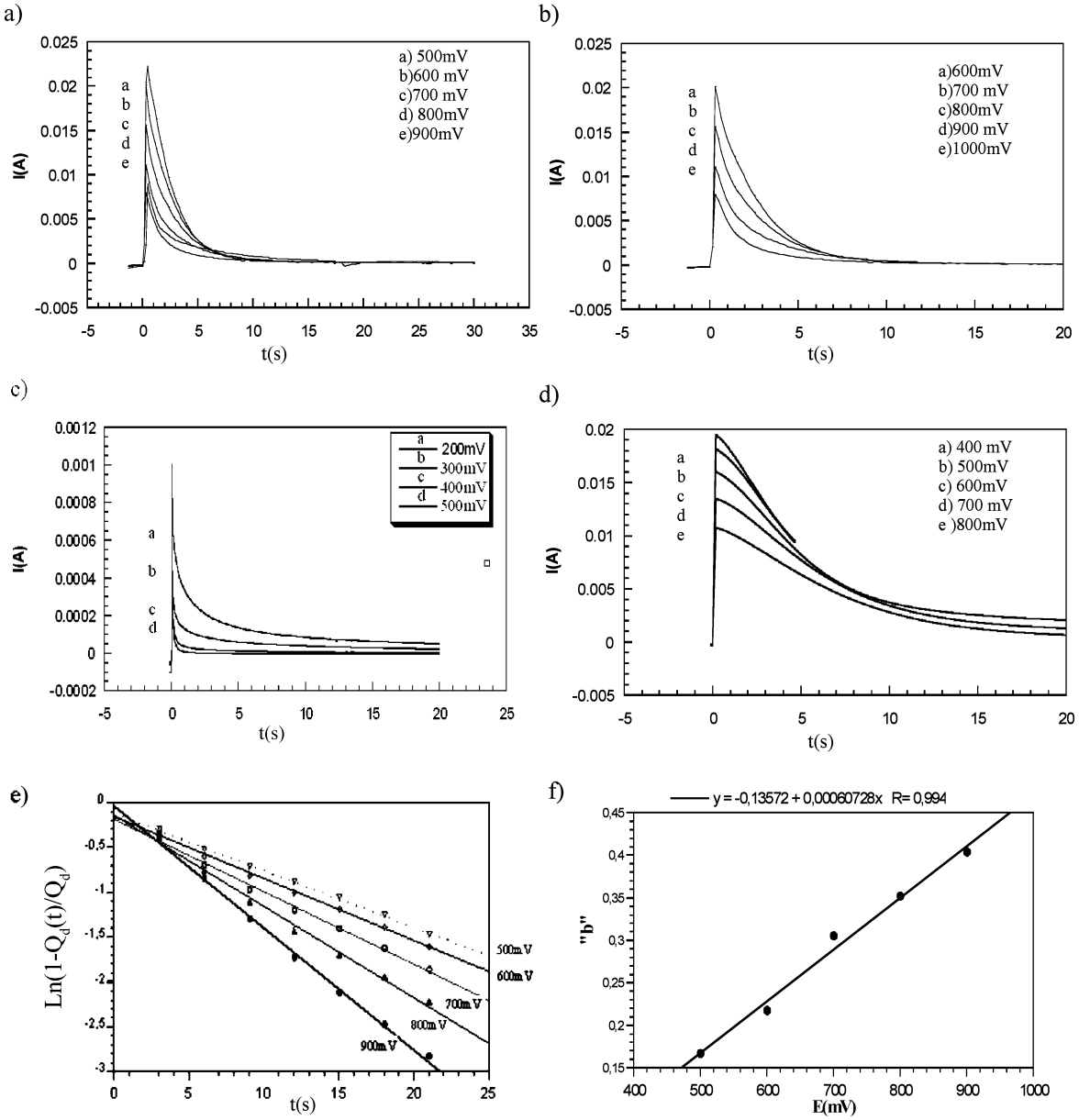

Figure 6. (a) Chronoamperograms of polythiophene film stepped from the same cathodic potentials of prepolarization (−200 mV) to different anodic limits (500, 600, 700, 800, and 900 mV) at constant temperature (25 °C) in 0.1 M $LiClO_4$/acetonitrile solution. (b) Chronoamperograms of poly(3-methylthiophene) film stepped from the same cathodic potentials of prepolarization (−500 mV) to different anodic limits (600, 700, 800, 900, and 1000 mV). (c) Chronoamperograms of poly(1-methylpyrrole) film stepped from the same cathodic potentials of prepolarization (−1400 mV) to different anodic limits (200, 300, 400, and 500 mV). (d) Chronoamperograms of polyaniline film stepped from the same cathodic potentials of prepolarization (800 mV) to different anodic limits (400, 500, 600, 700, and 800 mV). (e) Semilogarithmic plot of $1-Q(\tau)/Q$ vs oxidation time for a series of potential steps performed from −200 mV to different anodic values indicated in Figure 3a. Values of the difusional parameter *b* were obtained from the slopes for different applied anodic potentials. (f) Representation of the value of *b* as function of anodic potential for poly(3-methylthiophene).

TABLE 3: Values of *b* for Different Conducting Polymers

polymer	$b = f(E)$	E_0	b ($\eta = E - E_0 = 200$ mV)	D_{app} ($cm^2\,s^{-1}$)
polypyrrole	$0.45 + 0.67*E(V)$	−350 mV	0.35	8.47×10^{-11}
poly(1-methylpyrrole)	$0.18 + 0.32*E(V)$	−250 mV	0.16	3.87×10^{-11}
polyaniline	$0.074 + 0.002*E(V)$	150 mV	0.09	2.18×10^{-11}
polymethylaniline	$-0.066 + 0.27*E(V)$	200 mV	0.04	1.21×10^{-11}
polythiophene	$-0.22 + 0.8*E(V)$	300 mV	0.18	4.36×10^{-11}
poly(3-methylthiophene)	$-0.13 + 0.6*$E(V)	350 mV	0.07	1.69×10^{-11}

100 mV for polymethylaniline, 350 mV for polythiophene, and 400 mV for poly(3-methylthiophene). By performing potential steps from the above-mentioned reduction potentials for each polymer (kept for 60 s), to a potential 200 mV more anodic than the concomitant E_0 (η = constant), the experimental chronoamperograms allow those *b* and *D* constants to be obtained (depicted in Table 3). Values of the diffusion constant available in the literature for those polymers[34−43] range between 10^{-14} and $3.73\ 10^{-8}$.

The obtained diffusion coefficients shift for the studied families: polypyrrole > polythiophene > polyaniline. The obtained diffusion constants from methyl-substituted polymers

are about half of those obtained from nonsubstituted polymers. If the diffusion of counterions is slower, the kinetics of the oxidation process for this polymer and any electrochemical property (electrochromic, electromechanical, etc.) must be also slower.

Conclusions

Substituted polymers present more difficulties for the electrochemical stimulation of the conformational movements of chains, inducing more cathodic closing potentials (E_s) than those of the nonsubstituted polymers. Taking the closing potential as an indication of the electric work required to close the structure (current densities are very similar and small for all the studied polymers), the three studied families were classified by increasing values: polythiophene < polyaniline < polypyrrole.

This could be related to lower increments of the molar enthalpy (ΔH) during transition between two stationary states and lower diffusion constants due to slower swollen processes. The increment of the molar enthalpy between two stationary states defined under constant overpotentials of compaction and oxidation processes allows us to classify the studied families as: polyaniline < polythiophene < polypyrrole. ΔH values are always lower for the substituted polymers than the ΔH values for the nonsubstituted polymers from the same family. Greater ΔH values point to faster swollen processes giving greater diffusion constants, as was experimentally obtained.

The comparative treatment of different polymers by the ESCR model allows us, for the first time, to establish quantitative structural and thermodynamic magnitudes related to the electrochemical processes. Further studies in this direction would indicate new possibilities for the understanding, quantification, and optimization of the multiple properties and applications related to the electrochemistry of conducting polymers, such as artificial muscles, smart windows, and all solid polymeric batteries.

References and Notes

(1) Posey, F. A.; Morozumi, T. *J. Electrochem. Soc.* **1966**, *113*, 176−184.
(2) Aoki, K.; Tezuka, Y. *J. Electroanal. Chem.* **1989**, *267*, 55−66.
(3) Aoki, K.; Edo, T.; Cao, J. *Electrochim. Acta* **1998**, *43*, 285−289.
(4) Aoki, K.; Teragashi, Y.; Tokieda, M. *J. Electroanal. Chem.* **1999**, *460*, 254−257.
(5) Feldberg, S. W. *J. Am. Chem. Soc.* **1984**, *106*, 4671−4674.
(6) Yeu, T.; Nguyen, T. V.; White, R. E. *J. Electrochem. Soc.* **1988**, *135*, 1971−1976.
(7) Yeu, T.; Yin, K. M.; Carbajal, J.; White, R. E. *J. Electrochem. Soc.* **1991**, *138*, 2869−2877.
(8) Hillman, A. R.; Bruckensteis, S. *J. Chem. Soc., Faraday Trans.* **1993**, *89*, 3779−3782.
(9) Kaplin, D. A.; Qutubuddin, S. *J. Electrochem. Soc.* **1993**, *140*, 3185−3190.
(10) Kalaji, M.; Peter, L. M.; Abrantes, L. M.; Mesquita, J. C. *J. Electroanal. Chem.* **1989**, *274*, 289−295.
(11) Slama, M.; Tangui, J. *Synth. Met.* **1989**, *28*, C171-C176.
(12) Otero, T. F.; Rodríguez, J. In *Intrinsically Conducting Polymers: An Emerging Technology*; Aldissi, M., Ed.; NATO ASI Series; Kluwer Academic Publisher: Boston, MA, 1993.
(13) Otero, T. F.; Angulo, E. *Solid State Ionics* **1993**, *803*, 63−65.
(14) Baughman, R. H. *Synth. Met.* **1996**, *78*, 339−353.
(15) Jager, E. W. H.; Inganas, O.; Lundstrom, I. *Science* **2000**, *288*, 2335−2338.
(16) MacDiarmid, A. G.; Kaneto, K.; Saito, H.; Min, Y. *Polym. Mater. Sci. Eng.* **1994**, *71*, 713−714.
(17) Grande, H.; Otero T. F. *Electrochim. Acta* **1999**, *44*, 1893−1900.
(18) Otero, T. F.; Grande, H.; Rodríguez, J. *J. Electroanal. Chem.* **1995**, *394*, 211−216.
(19) Otero, T. F.; Grande, H.; Rodríguez, J. *Colloids Surf.* **1998**, *134*, 85−94.
(20) Otero, T. F.; Grande, H.; Rodríguez, J. *J. Phys. Org. Chem.* **1996**, *9*, 381−386.
(21) Otero, T. F.; Grande, H.; Rodríguez, J. *Synth. Met.* **1996**, *83*, 205−208.
(22) Otero, T. F.; Grande, H.; Rodríguez, J. *Synth. Met.* **1996**, *76*, 285−288.
(23) Otero, T. F.; Grande, H.; Rodríguez, J. *J. Phys. Chem. B* **1997**, *101*, 8525−8533.
(24) Otero, T. F.; Angulo, E. *Solid State Ionics* **1993**, *803*, 63−65.
(25) Otero, T. F.; Grande, H.; Rodríguez, J. *J. Phys. Chem. B* **1997**, *101*, 3688−3697.
(26) Odin, C.; Nechstchein, M. *Synth. Met.* **1993**, *55−57*, 1281−1286.
(27) Odin, C.; Nechstchein, M. *Phys. Rev. Lett.* **1991**, *67*, 1114−1117.
(28) Odin, C.; Nechstchein, M. *Synth. Met.* **1993**, *55−57*, 1287−1292.
(29) Inzelt, G.; Day, R. W.; Kinstle, J. F.; Chambers, J. Q. *J. Phys. Chem.* **1983**, *87*, 4592−4598.
(30) Grande, H.; Otero T. F. *J. Phys. Chem. B* **1998**, *102*, 7535−7540.
(31) Otero, T. F.; Grande, H.; Rodríguez, J. *Electrochim. Acta* **1996**, *41*, 1863−1869.
(32) Otero, T. F.; Boyano, I. *J. Phys. Chem. B* **2003**, *107*, 4269−4276.
(33) Otero, T. F.; Grande, H. *J. Electroanal. Chem.* **1996**, *414*, 171−176.
(34) Cai, Z.; Martín, C. R. *Synth. Met.* **1992**, *46*, 165−179.
(35) Genies, E. M.; Bidan, G.; Diaz, A. F. *J. Electroanal. Chem.* **1983**, *149*, 101−113.
(36) Penner, R. M.; Van Dyke, L. S.; Martín, C. R. *J. Phys. Chem.* **1988**, *92* 5274−5282.
(37) Ren, X.; Pickup, P. G. *J. Phys. Chem.* **1993**, *97*, 5356−5362.
(38) Herberg, B.; Pohl, J. P. *Ber. Bunsen-Ges.* **1988**, *92*, 1275−1279.
(39) Kim, J. J.; Amemiya, T.; Tryk, D. A.; Hashimoto, K.; Fujishima, A. *J. Electroanal. Chem.* **1996**, *416*, 113−119.
(40) Foot, P. J.; Mohammed, F.; Calvert, P. D.; Billingham, N. C. *J. App. Phys.* **1987**, *20*, 1354−1360.
(41) Mirebeau, P. *J. Phys., Colloq.*, **1983**, C3 579−582.
(42) Mohammad, F. *Synth. Met.* **1999**, *99*, 149−154.
(43) Kaneto, K.; Agaua, H.; Yashno, K. *J. Appl. Phys.* **1987**, *61*, 1197−1205.